

Supporting Information

Tailoring matter-orbitals mediated using nanoscale topographic interface for versatile colloidal current devices

Hyeonseol Kim^{1,†}, Yumin Kang^{1,†}, Byeonghwa Lim¹, Keonmok Kim¹, Jonghwan Yoon¹,
Abbas Ali¹, Sri Ramulu Torati^{1,*}, CheolGi Kim^{1,*}

¹*Department of Physics and Chemistry, DGIST, Daegu, 42988, Republic of Korea.*

*Corresponding authors: E-mail: srtorati@dgist.ac.kr (SR Torati) cgkim@dgist.ac.kr (CheolGi Kim)

†Equally contributed to the paper

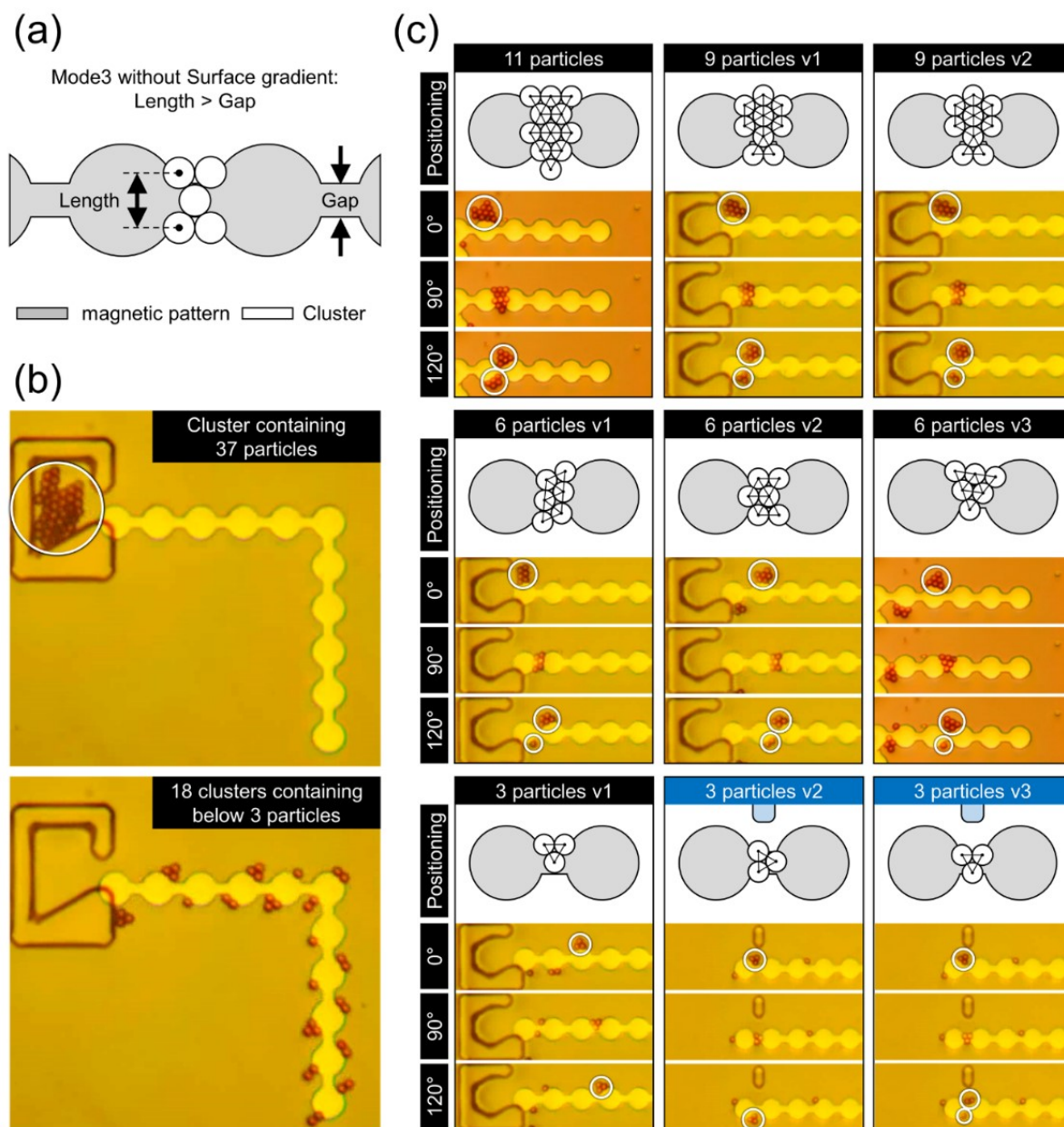


Figure S1. Stabilization effect of colloidal current by matter orbital. (a) Schematic representation of the structure of matter orbital and cluster of magnetic beads. (b) The stabilizing effect of cluster size when forced aggregated particles are released over the matter orbital. (c) The separation form of colloidal particle clusters by size in the gap. They tracked at 90° intervals. (version: v1-v3 represents the different splitting numbers at 120°)

Fig. S1 describes the stabilization process according to the number of particles. If the cluster is larger than the gap, the particles that made the cluster are captured in the two magnetic energy wells identified in Fig. 2b. To confirm this, we created a collecting room and aggregated 37 particles. When particles are taken out of the room, clusters of various sizes eventually separate into smaller chunks of three or less in the gap, as shown in Fig. S1c. When topographic effects are applied to matter orbital, they can be split into smaller particles, as shown in "3 particles v3" in Fig. S1c by Mode 3 in Fig. 2d.

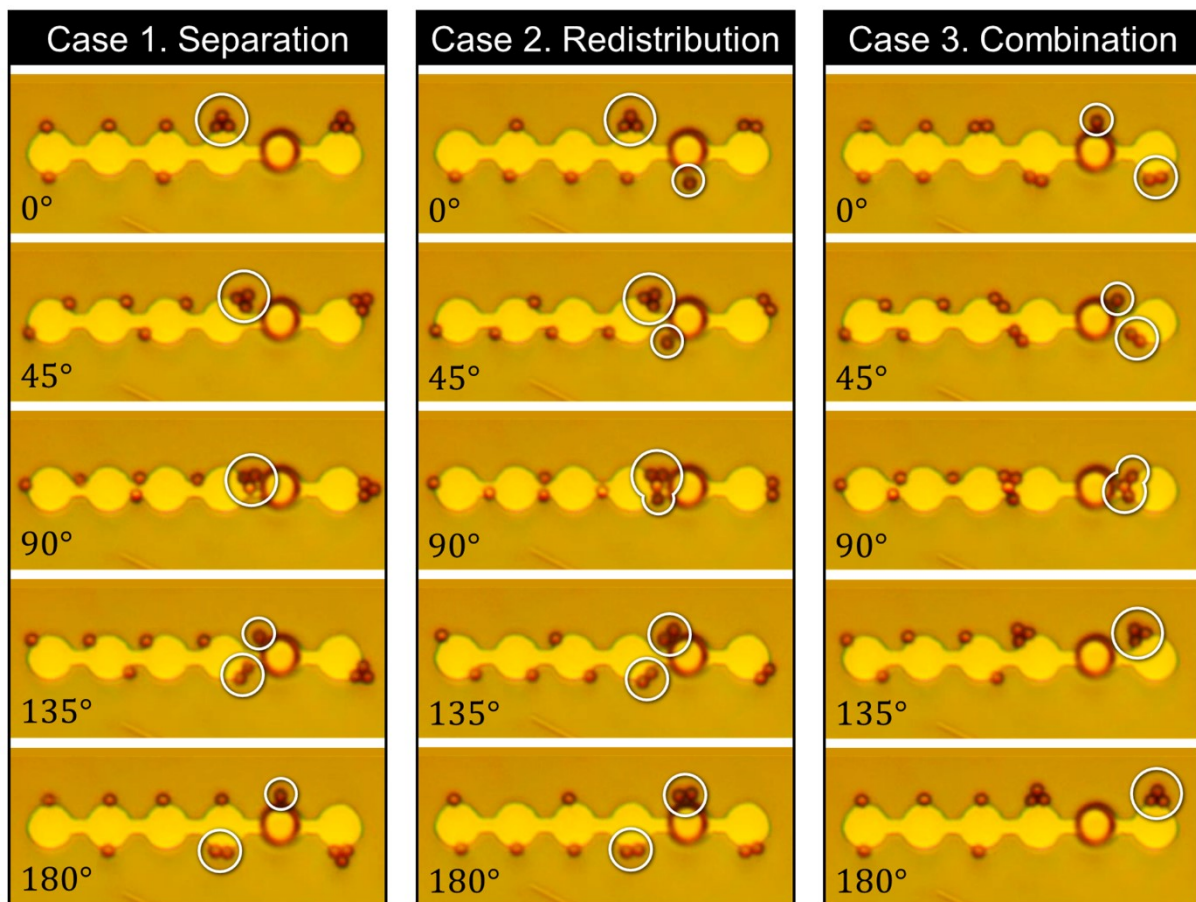


Figure S2. Irregularities of colloidal current by a pillar on the on-axis. Although the colloidal current is stabilized, gradients made in the same direction as the axis of the magnet pattern are randomly isolated, combined, and redistributed, resulting in unstable control.

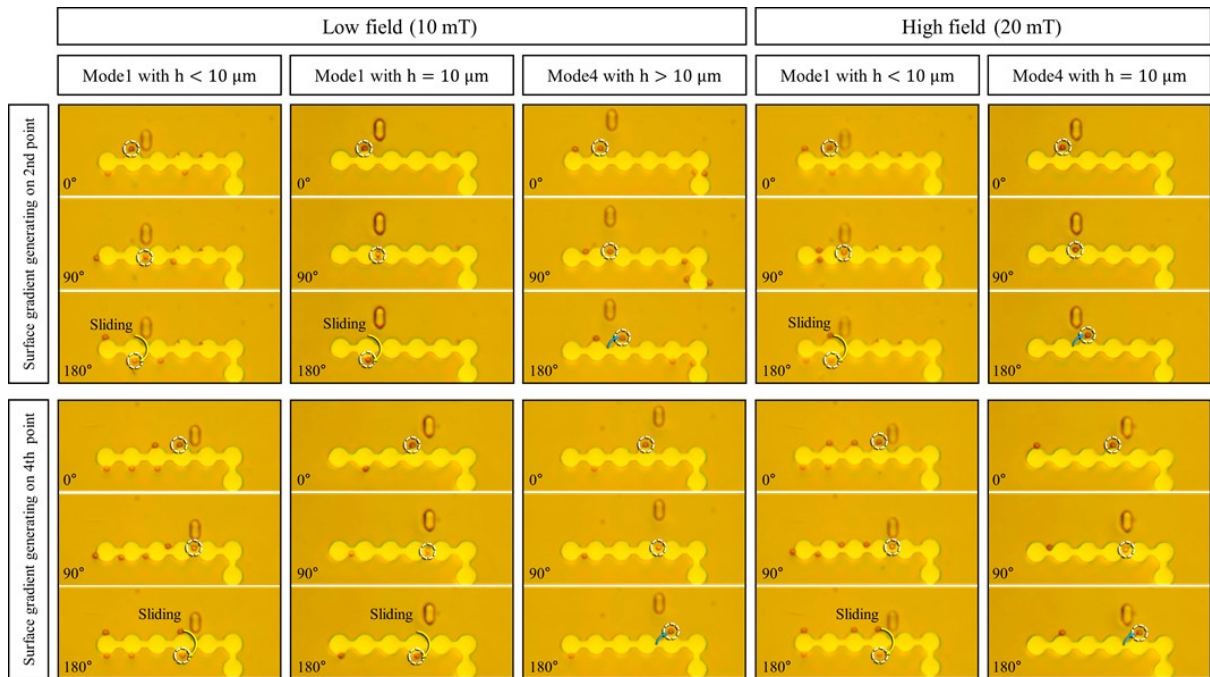


Figure S3. Various Modes of operation according to position and distance of pillar. "Micro hills" were fabricated for generating "surface gradient" on the 2nd and 4th switching points of the magnetic patterns at locations farther or closer than $10 \mu\text{m}$, respectively, away from the switching point. Mode1 and Mode4 were differently operated in each case depending on the distance between the "micro hill" and the magnetic pattern.

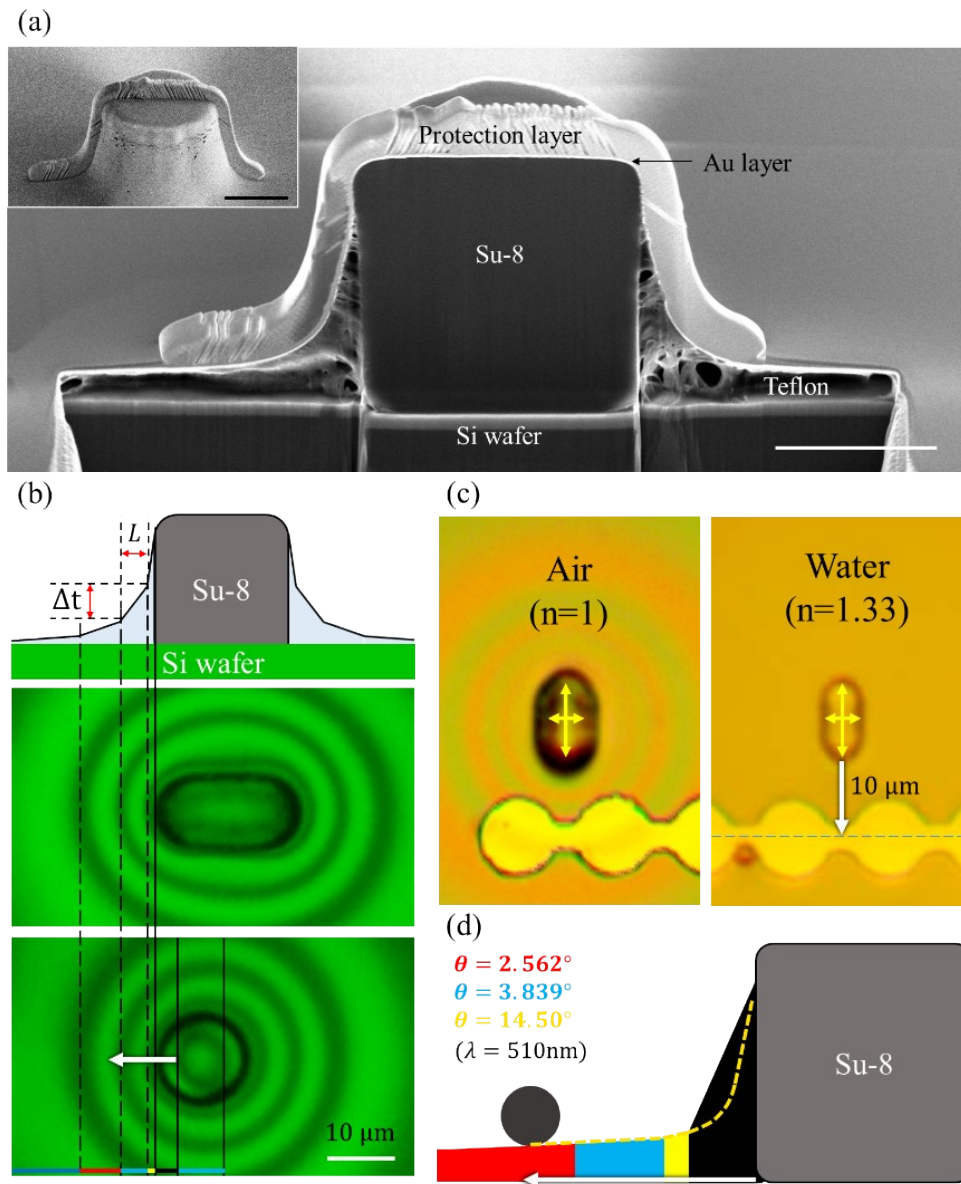


Figure S4. Surface gradient measurement using interference pattern ring and SEM. (a) Cross-sectional image of Teflon-coated "micro hill" by focused ion beam (FIB) technology (insert: an entire image of Teflon-coated "micro hill") (scale bar = 5 μm). (b) Interference fringes around the "micro hill" measured using irradiating light in wavelength range of 510–560 nm. The distance (L) between the adjacent interference patterns and height difference (Δt) were defined for calculating the gradient. (c) No interference patterns appear owing to the water layer in the experiment. Yellow arrows indicate the micrographic scale of "micro hill" underwater. (d) Cross-sectional diagram of "surface gradient" around the "micro hill" considering the calculated angle of gradient (θ). Locations of colored areas is matched with the position of the colored line (b). Yellow-dashed line is matched with the gradient line of the SEM image in (a). (b–d) White arrow indicate 10 μm.

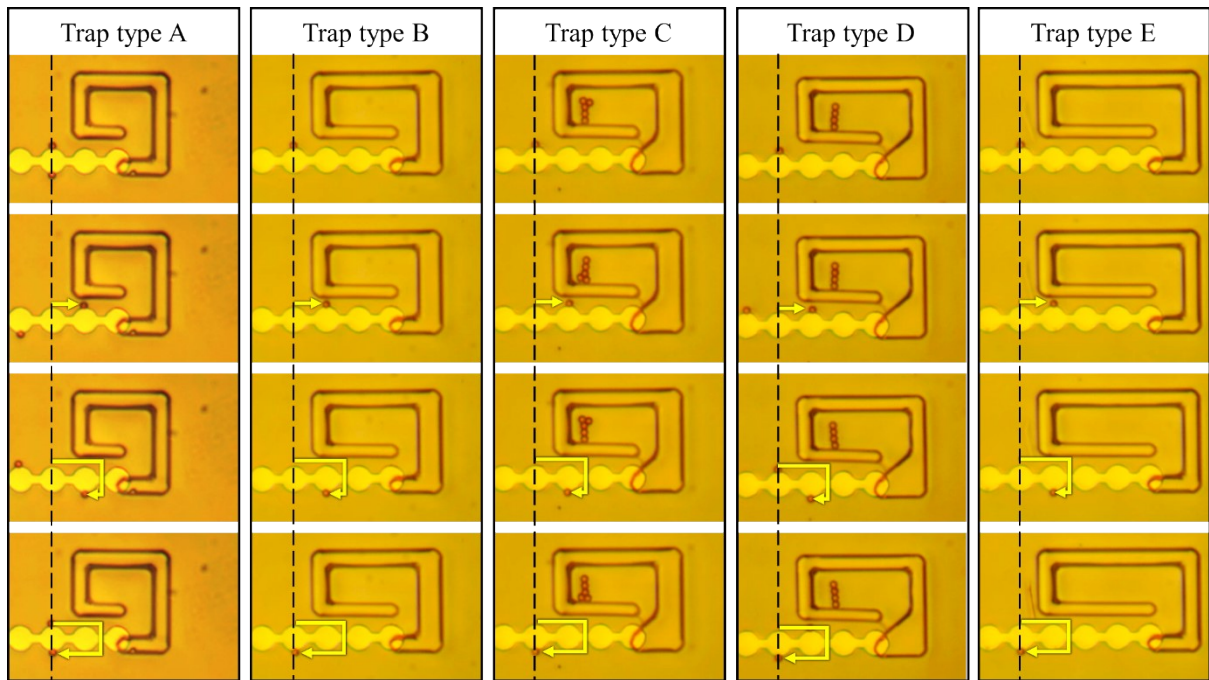


Figure S5. Mode1 performance is irrelevant with respect to complexity of the micro hill. Different types of "micro hill" structures were designed for trapping particles. Mode1 occurs at the same position, which is the 2nd switching point from the black-dashed line, owing to the equally generated "surface gradient" by structures regardless of length of trapping area and shape of structure on edge magnetic pattern.

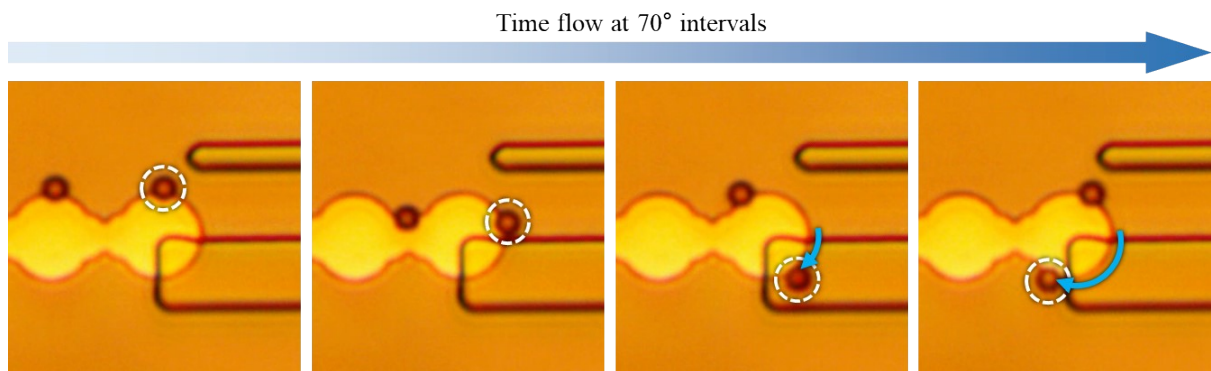


Figure S6. Magnetic bead ($2.8 \mu\text{m}$) that goes beyond a $3 \mu\text{m}$ -thick hill. While the particles follow an external rotating magnetic field, the particle crosses the "micro hill" with a relatively low height.

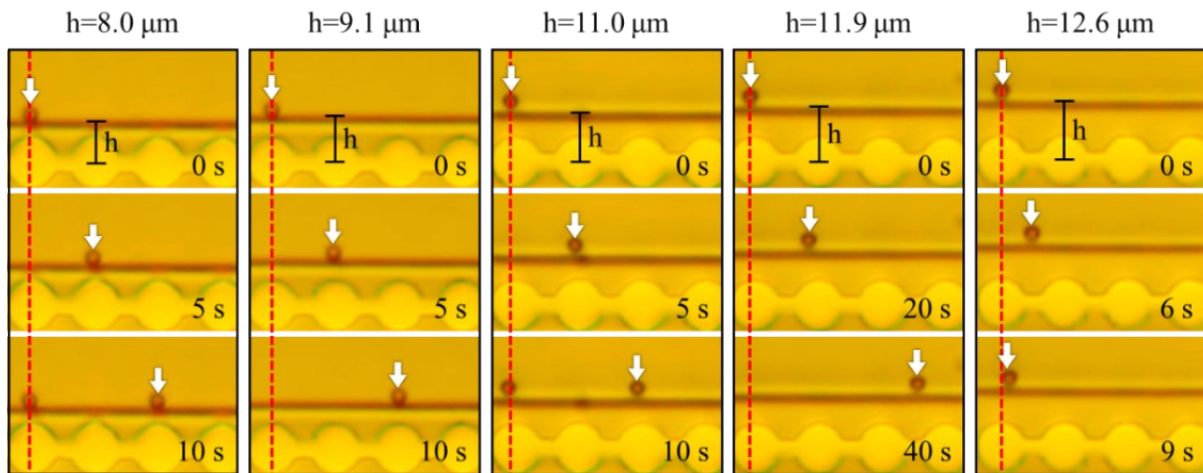


Figure S7. Transport of particles on the boundary of micro hill according to distance from the center of the disk-shaped pattern. Particles were transported along the boundary of "micro hill" under 0.1 Hz clockwise rotating magnetic field. When the distance (h) $<$ 11 μm , particles move at constant speed. However, with increasing h , the speed decreases, and the particles do not move toward the direction of progress.

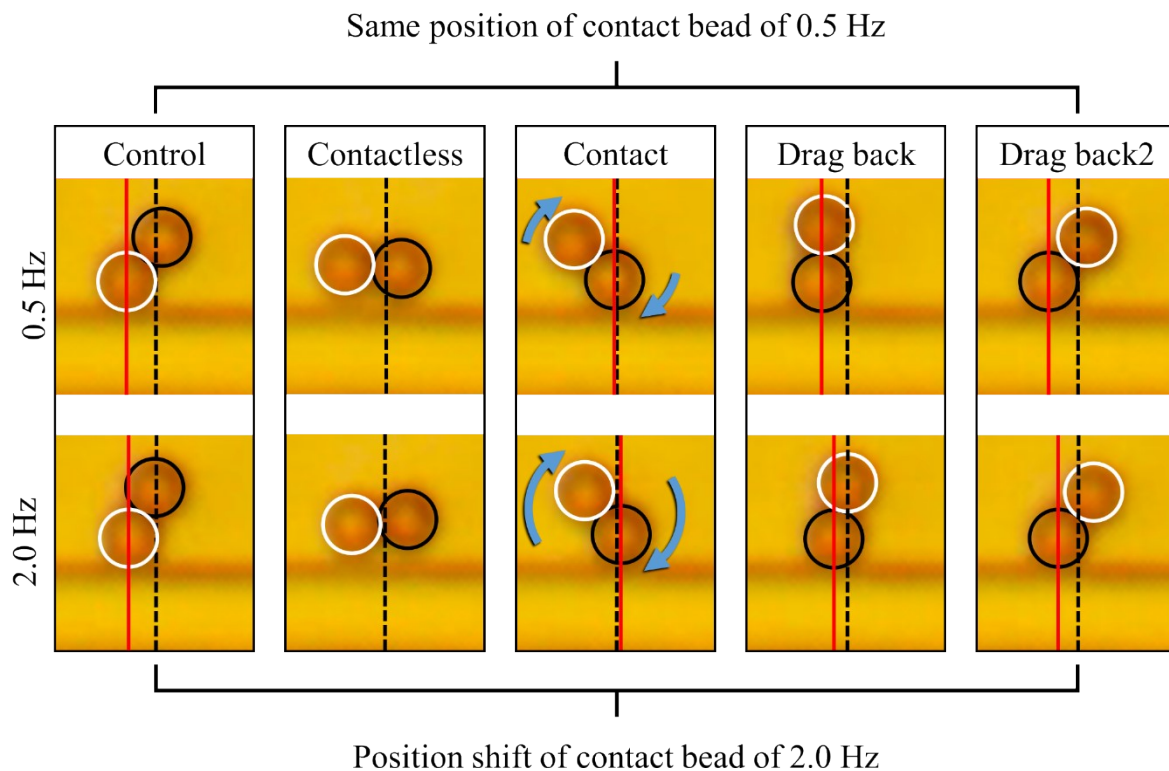


Figure S8. Comparison of position shift in particle chain according to rotating magnetic field frequency. The red line points to the center of the particle closer to the “micro hill,” and the black dashed line indicates the initial position. The particle chain undergoes a series of position shifts on the “micro hill” boundary under a rotating magnetic field. At low frequencies of the rotating field, the chain is more dragged to the back than at higher frequencies. Hence, the chain moves forward at a higher frequency.

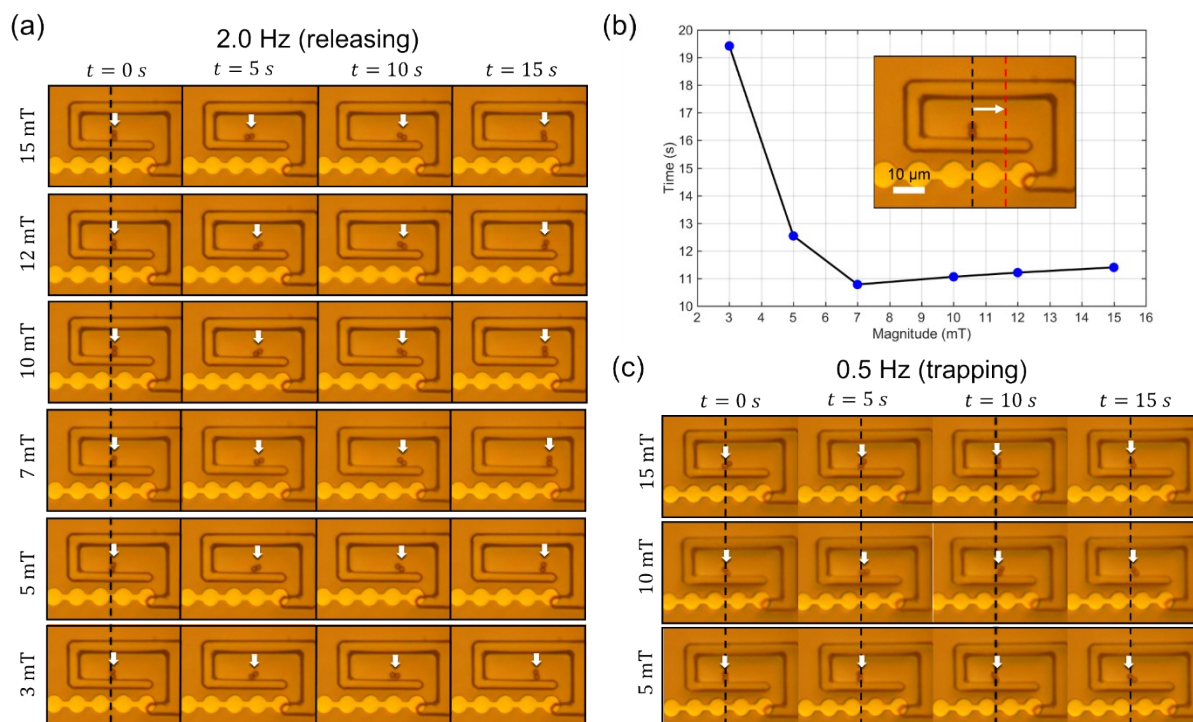


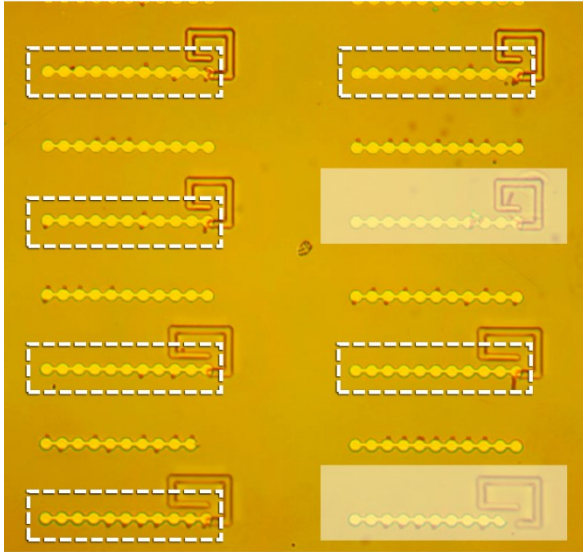
Figure S9. The movement of the chain according to the magnitude of the magnetic field.

(a) 2.0 Hz frequency of the magnetic field with releasing motion. (b) Releasing time difference at 2.0 Hz during 10 μ m from the initial equilibrium position. (c) 0.5 Hz frequency of the magnetic field with trapping motion.

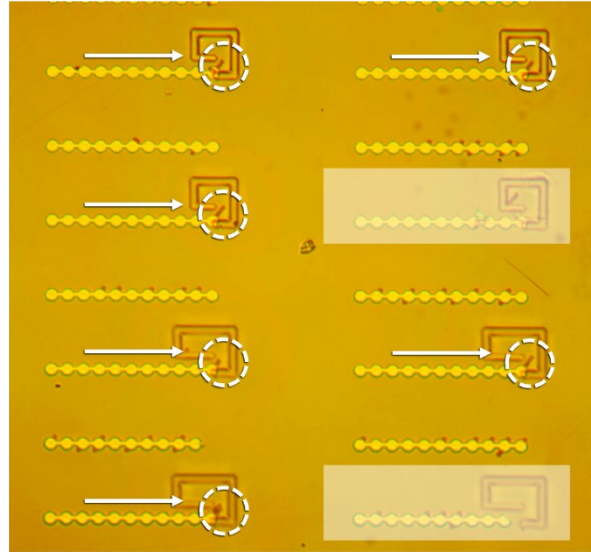
The releasing velocity is determined by the superiority of "walking motion" made by the rotating chain rubbing against the wall and "dragging" made by the matter orbital according to the change in the magnetic field (Fig. S6). The magnitude of the magnetic field is a factor that affects both motions. As the magnitude of the magnetic field increases, so does the "dragging" strength created by the matter orbital. During the "walking" process, it is involved in contact between particles and walls. Through experimental measurements, we found that when the external magnetic field is below 7 mT, the releasing speed increases as the field increases, and when it is greater than 7 mT, the releasing speed decreases slightly again (Fig. S9a and S9b).

The decrease in speed is due to reducing the wall contacts for "walking" while the chain rotates at the same frequency when the magnetic field is insufficient. In fields above 7 mT, the contact is stable, and the propulsion by rotation is constant, but the distance to drag back of Fig. S6 is increased due to the greater force generated by the matter orbital, which reduces the releasing speed. On the other hand, if the frequency is low, the chains have enough time to drag back to the equilibrium position, allowing them to be trapped at the initial position regardless of the magnitude of the magnetic field (Fig. S9c).

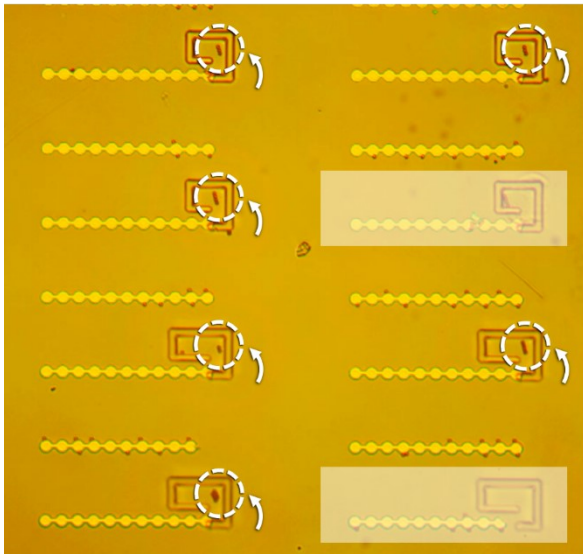
1. Initial state



2. Collect to Pre-zone



3. shift to trap



4. Trapping state

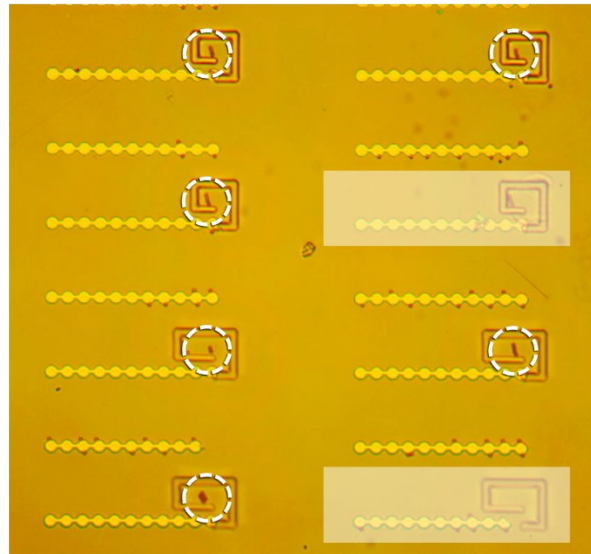


Figure S10. Simultaneous trapping of collected particles at pre-zone using Mode5. Targeted particles were collected at the pre-zone of each established trap room and simultaneously trapped despite the different initial positions of each targeted particle. The shift step using Mode5 for trapping does not affect the progress of non-targeted particles so that the non-trapped particles maintain their movements. After trapping, targeted particles are located in trap rooms as shown in trapping state. (White masked area: experimental error due to micromagnet pattern damaged or dust on the pattern)

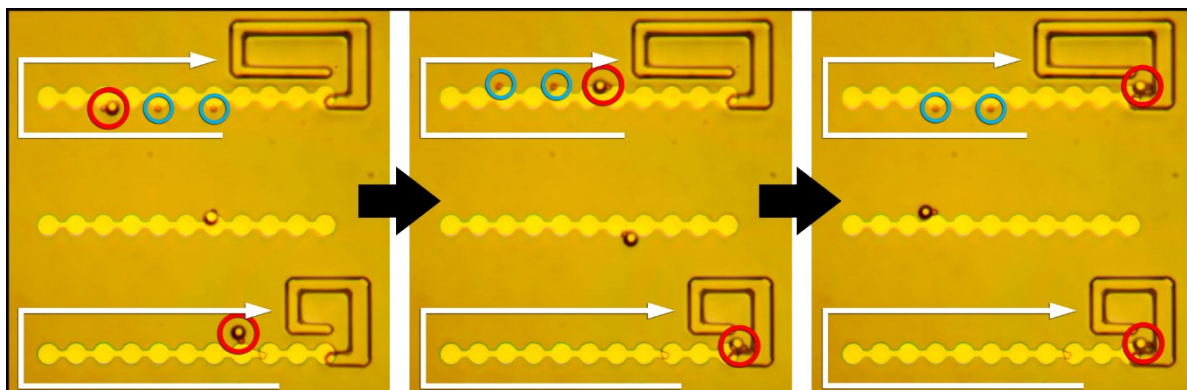


Figure S11. Absence of Mode1, which occurs by surface gradient for labeled particle. The "surface gradient"-induced "sliding" motion, named Mode1, for non-labeled particles. At the same operating condition, Mode1 does not occur for the labeled particle while the non-labeled particles are continuously in "sliding" motion.

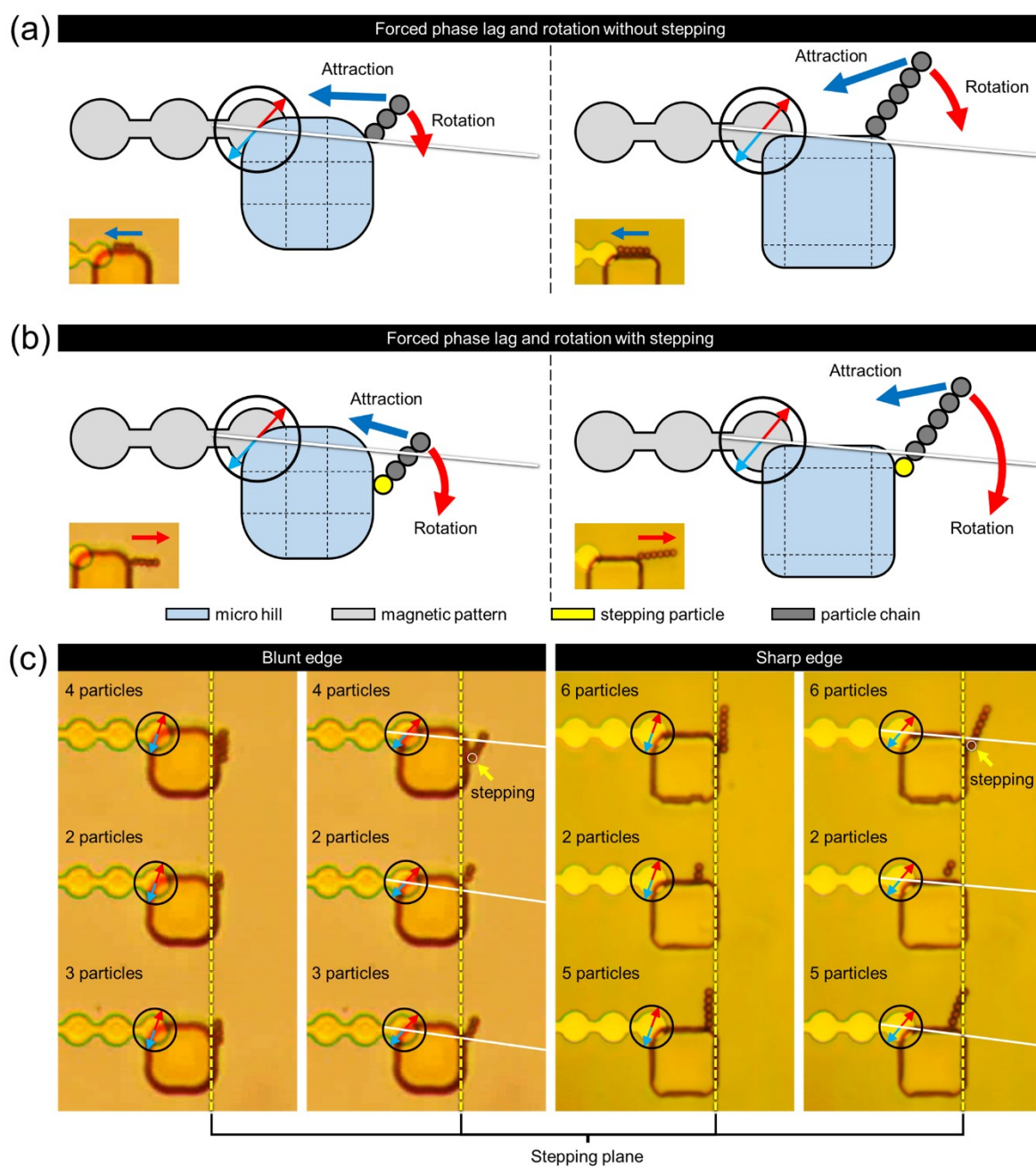


Figure S12. Threshold effect of Colloidal current by Forced phase lag. (a) Forced phase lag, rotation without stepping, and (b) with stepping. (c) Create stepping particles in chains of different lengths for each pillar shape. Although it is a square pillar of the same size, the dynamics of the colloidal current vary depending on whether it has a blunt or sharp edge.

Generally, a magnetic particle chain in a free space rotates along the direction of the magnetic field and maintains its position. However, suppose there is a micro-magnet in the vicinity. In that case, the chain's position is in the attractive zone from the magnetization direction of the magnet, and it is dragged toward the matter orbital (Fig. 2a and 2b).

At that time, the square pillar with different curved edges could apply the threshold effect to

the colloidal current, which moves continuously along the matter orbital. Depending on whether the pillar has a blunt or sharp edge in unconnected matter orbital, a certain number of particles could be collected and then jumped to an adjacent matter orbital (Fig. S12). The pillar becomes a kind of stepping plane. The rotation of the particle chain along the magnetic field direction and the attractive force created by the matter orbitals desire to move the chain in opposite directions. At this moment, as shown in Fig. S12b, if the chain steps on the stepping plane even though the chain is parallel to the matter orbital, it can enter the repulsive zone again due to physical interference of the pillar without being dragged, as shown in the insert figure of Fig. S12a. As a result, the chain starts jumping toward the adjacent matter orbital. This movement could delay the flow of the colloidal current until a particular value of colloidal current particles was collected, like the current or voltage threshold effect in semiconductors.

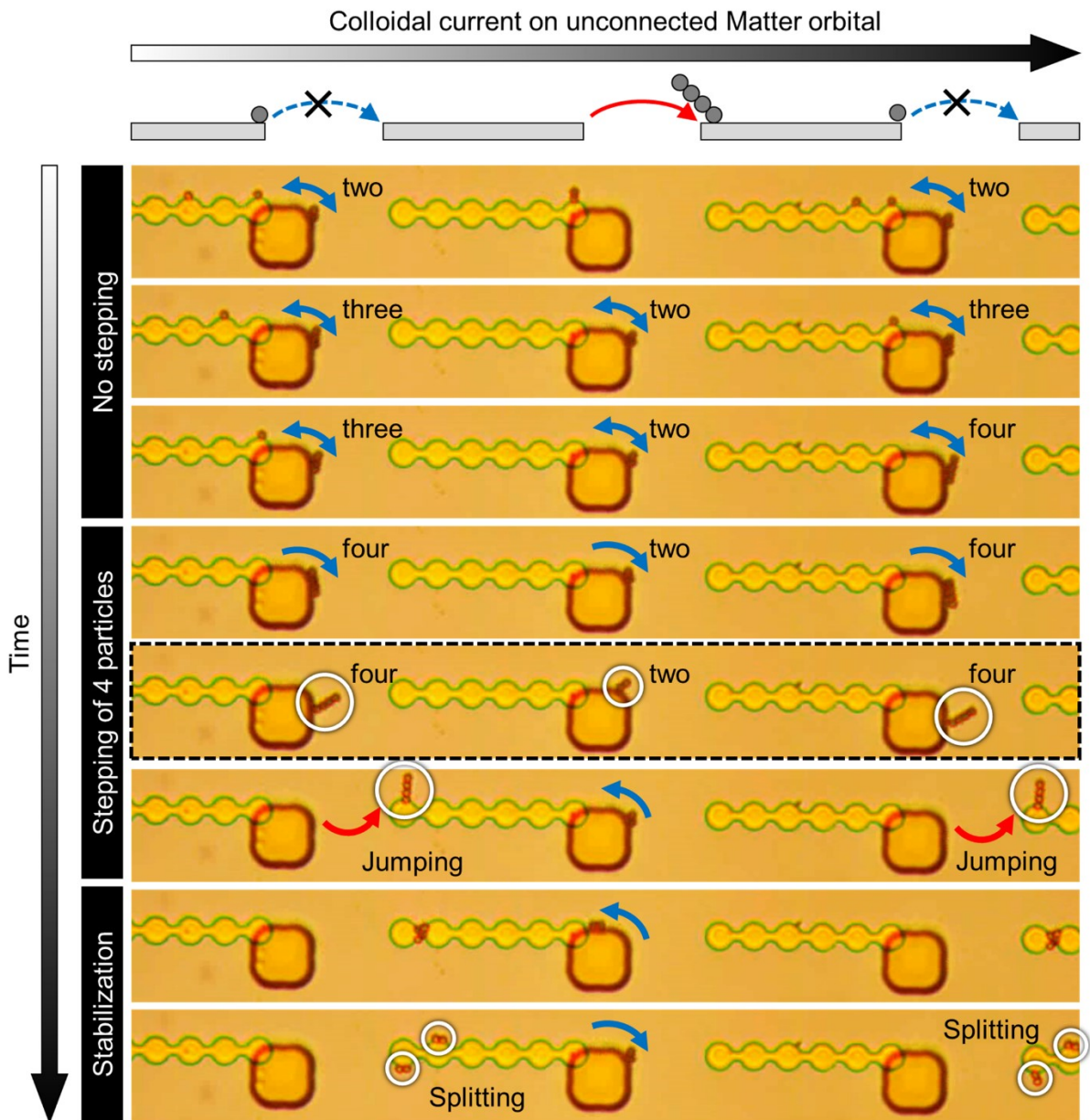


Figure S13. Threshold effect of Colloidal current on unconnected matter orbitals. The colloidal current particles were collected on the square pillar until forming one chain including four particles. The chain stepped the stepping plane and jumped to the adjacent matter orbital. After reaching the next matter orbital, it was split by the stabilization effect.

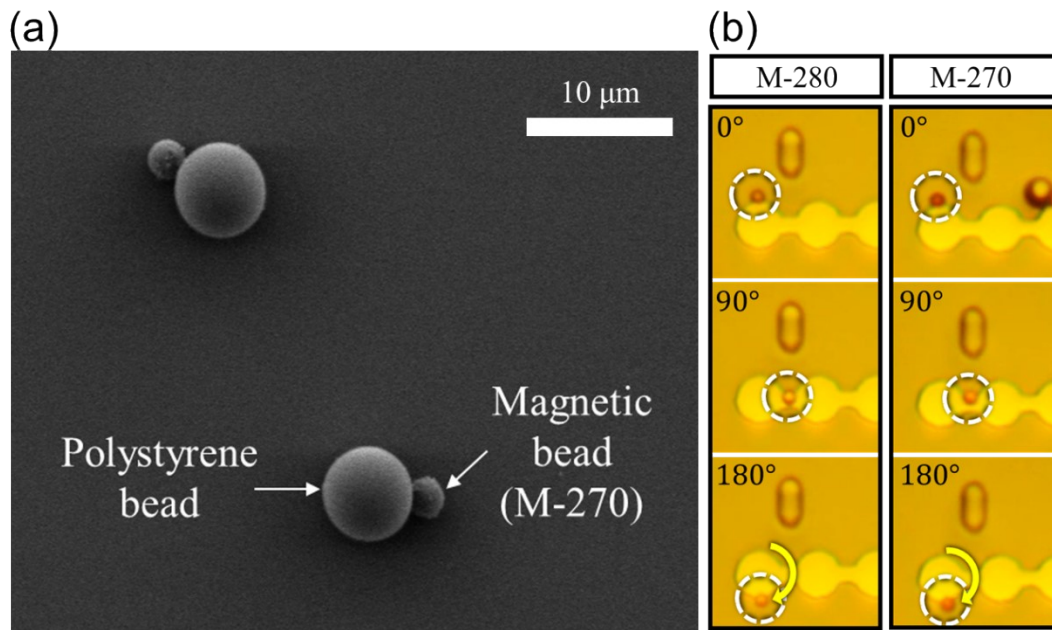


Figure S14. Labeled particles and dynamics of two superparamagnetic particles. (a) SEM image of colloidal particles. (b) Same particle dynamics with less to do with the magnetic properties of the particles.

In actual experiments, we used particles of M-270 carboxylic acid and M-280 streptavidin with the same size but different magnetic properties and surface coatings. In both cases, the same results could be obtained from dynamics by topographic effects (Fig. S14b). This result supports that there is only a slight difference in the magnitude of magnetic energy, and there is no significant difference in the shape of the energy distribution, shown in Fig.2c, that moves the particles by considering that the two particles have superparamagnetic properties.

Supporting Movies

Movie S1: Matter-orbital mediated topographic effects that mimic electron system #1

Movie S2: Matter-orbital mediated topographic effects that mimic electron system #2

Movie S3: Orbital departure by forced phase owing to micro-hill and corresponding device #1

Movie S4: Orbital departure by forced phase owing to micro-hill and corresponding device #2

Movie S5: Return to orbital by rotation frequency and integrated device with Mode switching

Movie S6: Selective manipulation by external magnetic field control with Mode switching